Mathematical and Computer Modelling 51 (2010) 944–955

Contents lists available at ScienceDirect

Mathematical and Computer Modelling

journal homepage: www.elsevier.com/locate/mcm

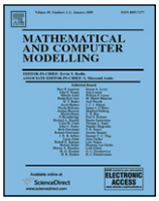

Simulation-based evolutionary method in antenna design optimization

Yiming Li

Institute of Communication Engineering, National Chiao Tung University, Hsinchu 300, Taiwan
Department of Electrical Engineering, National Chiao Tung University, Hsinchu 300, Taiwan
National Nano Device Laboratories, Hsinchu 300, Taiwan

ARTICLE INFO

Keywords:
Optimization
Genetic algorithm
Numerical electromagnetic method
Antenna
Maxwell's equations
Finite element method

ABSTRACT

In this paper, a simulation-based optimization method for the design of antenna patterns in mobile broadcasting, multi-bandwidth operation and the 802.11a WLAN is presented. The simulation-based genetic algorithm (GA) is advanced for the antenna design automation with requested specifications. The corresponding cost function in optimization is evaluated by an external numerical electromagnetic (EM) solver, where the communication between the GA and EM solver is implemented with our unified optimization framework (UOF). An A Z-shaped antenna is explored as an example to express the optimization methodology with respect to the specific return loss. Inspired by the scenario of GA for the optical proximity correction in our earlier work, we firstly partition the edges of the antenna into small segments, and then adjust the movements of each segment to construct a newer geometry for the designed antenna with a better return loss. The external EM solver is then performed to calculate the return loss of the newer antenna. The optimized antenna pattern is achieved when the simulated results meet the specific constraints, and then UOF exports the antenna pattern with the better return loss evaluated by the external EM solver. Otherwise, the evolutionary algorithm will enable us to search for a better solution again. UOF presents the capability in the optimization with an external solver. Our preliminary numerical results confirm the robustness and efficiency of the developed simulation-based optimization method.

1. Introduction

A trend of portable device integration has arisen in last decade, due to the massive growth of wireless communications, and products are expected to have multiple wireless service. As a result, a single, small antenna with the ability to operate effectively over each required bands, is desired. Modern antenna applications have special specifications, such as small size, multi-band, broadband requirement, beam-forming, high system gain and so on, in communication systems [1–14]. In the past years, in order to achieve the desired specifications based on well-known geometry, how to adjust the geometry to get the best design has been a state-of-art, and needs more experience through trial-and-error process. Recently, the optimization scheme, genetic algorithm (GA) [15–21], is considered to be a efficiency approach to optimize the antenna to satisfy requested specifications and make design procedure fully automatic [1–14]. Based on pre-selected design parameters, such as the geometry dimensions [1,3,8–12], loads locations and the corresponding values [1,11], the number of elements of fractals [2,5,6], the number of antenna arrays [3,12], the existence of discretized patterns [4,7], and so on, GA adjusts those antennas automatically and communicates with full-wave electromagnetic solvers to evaluate the cost function. The GA-based optimized dual-band antenna has been studied by many research groups [4,7,9,10], and could be divided into two different approaches. One starts from a rectangular antenna with its geometry discretizing into sequential uniform elements, and then GA is used to decide which elements are reserved or removed from the geometry [4,7]. The optimized antenna

E-mail address: ymli@mail.nctu.edu.tw.

0895-7177/$ – see front matter
doi:10.1016/j.mcm.2009.08.017

consists of those reserved elements. The other approach uses the parts of geometry as the parameters in the optimization procedure, such as the patch length, width, etc., and then automatically tunes those values [9,10]. As far as we know, the notch and slit-loaded entries provide extra resonant frequencies and introduce a new band into the original antenna [22]. Hence the approach in [4,7] works well, but their ability depends on the grid's size. Recently, the wire antenna optimization using GA has been studied [23]. However, such bending approach cannot be used in planer antenna design. To make GA more flexible in planer antenna design optimization, we provide a new approach to optimize the planer antenna.

In this work, we implement an optimization method to enhance the receiving and transmitting abilities of the given antenna with GA and numerical simulation. Based on our experience and technique of using GA to optical proximity correction (OPC) [24–26], transistor model parameter extraction [27,28] and doping profile optimization [29], we, for the first time, advance the idea of pattern correction in OPC for antenna design optimization. The proposed method partitions the edges of the antenna into some sections (small segments), and then those sections can be shifted in the normal direction of the edges to improve the return loss of the antenna. This novel approach means the variation of geometry has more freedom than the two approaches mentioned above. It can extend the geometry without limited boundaries and can construct geometry without specific form. The involved simulator solves the Maxwell's equations by finite element method. The Maxwell's equations govern the performance in electric and magnetic fields, and the simulated results are applied to evaluate the newly generated antenna. A Z-shaped antenna is used in our examination, which has radiation elements and a ground plane on the same plane, and it has only one clear band. To enhance the second band, we try to add the discontinuities for current on the patch (i.e., change the geometry of the antenna). Both the accuracy and computational efficiency show that the evolved antenna satisfies the specification.

The paper is organized as follows. In Section 2, we briefly introduce the finite element method for the numerical solution of the adopted Maxwell's equations. In Section 3, the procedure of the GA-based optimization method is stated in details. In Section 4, results and a discussion are given. Finally, we draw conclusions and suggest future work.

2. The finite element method for electromagnetic problem in antenna design

In this section, we state the Maxwell's equations which are fundamental in electromagnetics [30]. The Maxwell's and continuity equations in the differential form are

$$\nabla \times \mathbf{E} = -\frac{\partial \mathbf{B}}{\partial t}, \tag{1}$$

$$\nabla \times \mathbf{H} = \frac{\partial \mathbf{D}}{\partial t} + \mathbf{J}, \tag{2}$$

$$\nabla \cdot \mathbf{D} = \rho, \tag{3}$$

$$\nabla \cdot \mathbf{B} = 0, \tag{4}$$

and

$$\nabla \cdot \mathbf{J} = -\frac{\partial \rho}{\partial t}, \tag{5}$$

where $\mathbf{E}$ is electric field intensity, $\mathbf{D}$ is electrical flux density, $\mathbf{H}$ is magnetic field intensity, $\mathbf{B}$ is magnetic flux density, $\mathbf{J}$ is electric current density, and ρ is electric charge density. The bold face denotes vectors. Consider that the time-harmonic Eqs. (1), (2) and (5) can be rewritten in the following forms

$$\nabla \times \mathbf{E} = -j\omega\mathbf{B}, \tag{6}$$

$$\nabla \times \mathbf{H} = j\omega\mathbf{D} + \mathbf{J}, \tag{7}$$

and

$$\nabla \cdot \mathbf{J} = -j\omega\rho, \tag{8}$$

where $\omega = 2\pi f$, and f is the operation frequency. Based on the time-harmonic case with constitutive relations, the vector wave equations can be derived as

$$\nabla \times \left(\frac{1}{\mu_r}\nabla \times \mathbf{E}\right) - \omega^2\mathbf{E} = -j\omega\mathbf{J}, \tag{9}$$

$$\nabla \times \left(\frac{1}{\varepsilon_r}\nabla \times \mathbf{H}\right) - \omega^2\mu_r\mathbf{H} = \nabla \times \left(\frac{\mathbf{J}}{\varepsilon_r}\right), \tag{10}$$

where ε_r is the premitivity and μ_r is the premiability. Now we introduce how to apply the finite element method (FEM) to solve Maxwell's equations for the antenna design problem. To derive the FEM formulations, first we consider the boundary value problem in three-dimension (3D) with the general form

$$-\frac{\partial}{\partial x}\left(\alpha_x\frac{\partial \phi}{\partial x}\right) - \frac{\partial}{\partial y}\left(\alpha_y\frac{\partial \phi}{\partial y}\right) - \frac{\partial}{\partial z}\left(\alpha_z\frac{\partial \phi}{\partial z}\right) + \beta\phi = f, \forall (x, y, z) \in V, \tag{11}$$

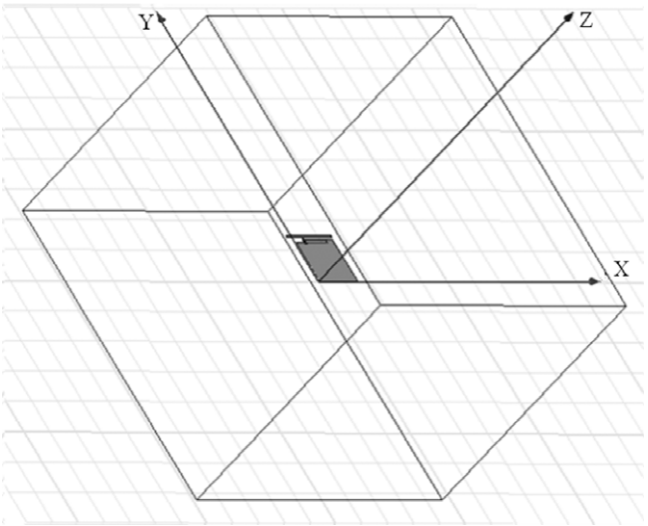

Fig. 1. An illustration of the problem domain for the examined antenna (gray area). For the studied structure of the antenna, the upper line presents the ground plane and the lower rectangle behaves as the radiation element.

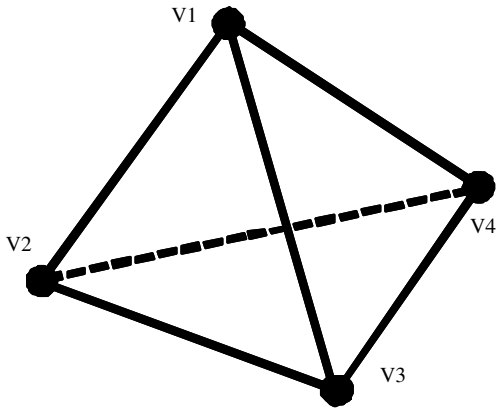

Fig. 2. The linear tetrahedral element. The labels for four nodes are local indices in FEM.

and the boundary conditions are $\phi = p$ on S_1 and

$$\left(\alpha_x \frac{\partial \phi}{\partial x}\hat{x} + \alpha_y \frac{\partial \phi}{\partial y}\hat{y} + \alpha_z \frac{\partial \phi}{\partial z}\hat{z}\right) \cdot \hat{n} + \gamma\phi = q, \tag{12}$$

on S_2. ϕ denotes the unknown function, V is the simulation domain, S_1 is the surface with the Dirichlet boundary condition, S_2 is the surface with the boundary condition of the third kind, and other parameters are known when converting the physical problem into the boundary value problem. In our examined antenna case, as shown in Fig. 1, the antenna with dimension 30 mm × 30 mm (gray area) is surrounded by the cubic with dimension 190 mm × 190 mm × 160 mm. The boundary conditions of all the edges, such as absorbing boundary condition (ABC) [31–33], perfectly matched layer (PML) [34,35], etc., satisfy the third kind boundary condition.

The corresponding variational problem for above boundary value problem is

$$\frac{\partial F(\phi)}{\partial \phi} = 0, \tag{13}$$

where

$$F(\phi) = \frac{1}{2}\iiint_V \left[\alpha_x \left(\frac{\partial \phi}{\partial x}\right)^2 + \alpha_y \left(\frac{\partial \phi}{\partial y}\right)^2 + \alpha_z \left(\frac{\partial \phi}{\partial z}\right)^2 + \beta\phi^2\right] \mathrm{d}V + \iint_{S_2} \left(\frac{\gamma}{2}\phi^2 - q\phi\right) \mathrm{d}S - \iiint_V f\phi \mathrm{d}V, \tag{14}$$

and $F(\phi)$ is named functional. The unknown function can be obtained by solving Eq. (14). To compute the solution, FEM is applied. FEM first discretizes the 3D simulation domain using tetrahedral elements and calculates the expression of the

unknown function on each element. For example, Fig. 2 shows a linear tetrahedral element, which uses four vertices V1, V2, V3, and V4 as the basis to represent the electric and magnetic field within the element. It mimics the unknown function as

$$\phi^e(x, y, z) = a^e + b^e x + c^e y + d^e z, \tag{15}$$

where the superscript e denotes the region of each discretized element. After discretization, Eqs. (13) and (14) can be transferred into the matrix form such as

$$\begin{aligned}\left\{\frac{\partial F(\phi)}{\partial \phi}\right\} &= \sum_{e=1}^{M}\left\{\frac{\partial \overline{F^e}(\phi^e)}{\partial \phi^e}\right\} + \sum_{s=1}^{M_s}\left\{\frac{\partial \overline{F_b^s}(\phi^s)}{\partial \phi^s}\right\} \\ &= \sum_{e=1}^{M}\left(\left[\overline{K}^e\right]\left\{\overline{\phi}^e\right\} - \left\{\overline{b}^e\right\}\right) + \sum_{s=1}^{M_s}\left(\left[\overline{K}^s\right]\left\{\overline{\phi}^s\right\} - \left\{\overline{b}^s\right\}\right) = \{0\}. \end{aligned} \tag{16}$$

In the above expression, $\{A\}$ denotes a column vector, $[A]$ denotes a matrix, e is the entry corresponding to discretized element, superscript s denotes the entry corresponding to surface, M represents the total discretized elements inside the simulation domain, M_s denotes the total elements on the boundaries of the simulation domain, and the bar over entries in the equation denotes the global representation which transfers from the local representation without bar. Finally, the solution will be obtained by solving the Eq. (16). Comparing Eq. (11) with Eqs. (9) and (10), the parameters in Eq. (11) can be extracted. Also, the boundary conditions and the continuity of fields between two materials in the electromagnetic problem can also be related to Eq. (15) and (16). For open structures, in order to truncate the problem into the finite domain, ABC and PML are used to model the boundary conditions and to avoid the reflection at artificial boundaries [30–35]. The radiation pattern and the return loss are then evaluated to show the antenna property [36].

3. The intelligent methodology

As a designer drew a blueprint of an antenna for the specific purpose, a fine tune process should be performed repeatedly for further improvement. We already know the geometry of the antenna affects its performance. However, the major difficulty is how the antenna shape affects its performance. For an antenna designer, when one fine tunes the shape, it is just like making a wild guess. To automate the search for the optimized antenna shape in an efficient way, GA is a good candidate of optimization methods in the simulation-based procedure. Fig. 3 shows the flowchart of the proposed optimization approach. During the procedure, the original antenna shape is divided into small segments. The movements of those segments are then optimized with respect to the calculated results, using GA. Then the GA is applied to correct the antenna shape and outputs a new geometry of antenna. To evaluate the cost function in GA, the external EM solver is used to simulate the new antenna. This procedure will continue until all the specifications are satisfied by the optimized antenna. We have implemented this optimization procedure in our developed unified optimization framework (UOF) [15,16]. UOF has already provided an efficient way in OPC problem using a simulation-based optimization scheme. Based on such a successful experience, we now extend the idea to do the simulation-based antenna optimization. There are several components in the GA [15–19], such as problem definition, encoding method, fitness evaluation, selection method, and crossover procedure, and a mutation scheme has to be performed for an evolutionary process. A computational procedure for the implemented GA in the optimal antenna design problem is shown below.

```
GA with antenna design problem
Begin
  Partition edges of antenna into segments
  For j = 1 to Number of segments
    GeneEncode(Segment[j])
  End For
  While ErrorNorm does not satisfy the stop
criteria
    Evolution()
    UpdateSegment()
    return_loss(optimized) = External EM
Solver(CorrectedShape)
    ErrorNorm
= return_loss(optimized) − return_loss(original)
  End While
  Output optimized antenna
End
```

The combination of simulation-based intelligent antenna optimization and GA adopts GA as an optimizer to search for the best movement of each segment and to then produce an optimized shape. The implementation of each procedure in the proposed GA is described as follows.

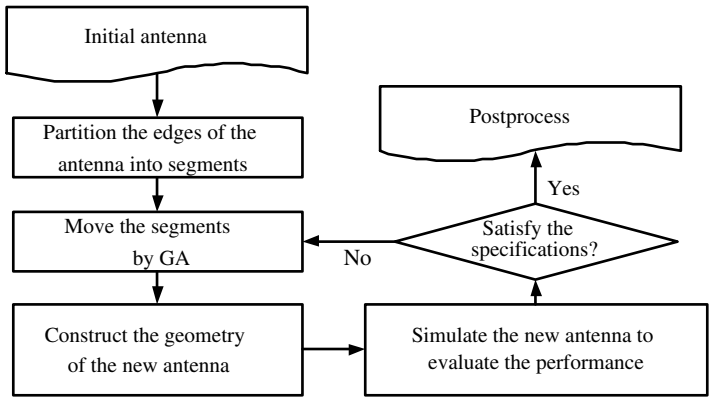

Fig. 3. A flowchart for the proposed optimization approach in antenna design.

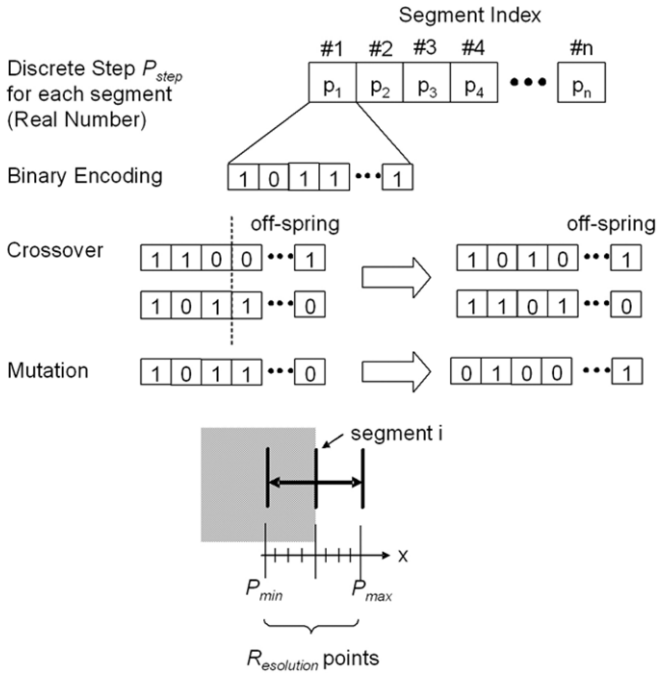

Fig. 4. Encoding method for the antenna optimization problem and crossover and mutation operation.

(1) Problem Definition

Our goal in the antenna design problem is to obtain an optimized antenna whose geometry produces the improved return loss within the requested frequency bandwidth. It means that the GA will find out the best configuration of the antenna shape, and the extracted return loss of the optimized antenna is less than the return loss of the original antenna within such bandwidth. In the antenna optimization, the relationship between specification, corrected shape, their return losses and errors can be written as follows:

Specification: $Return\_loss(goal)|_{f_i}$;
Corrected Shape: CS;
Return loss: $Return\_loss(optimized)$ = External EM Solver(CS); and
Error: $Err = \sum_{i=1}^{N_f} \left(Return\_loss(optimized)|_{f_i} - Return\_loss(goal)|_{f_i}\right)$;

where the $Return\_loss(goal)|_{f_i}$ is the return loss at the specified frequency f_i, and N_f denotes the total number of specified frequencies. In this work, the external EM solver, such as HFSS [37], FEKO [38], IE3D [39], etc. is used to solve the return loss of the antenna.

(2) Encoding Method

The encoding method is the procedure that encodes the target parameters into genes. In the proposed method, we encode the movements of each segment into genes. For example, in the chromosome $P_1P_2P_3P_4$, the genes P_1, P_2, P_3, and

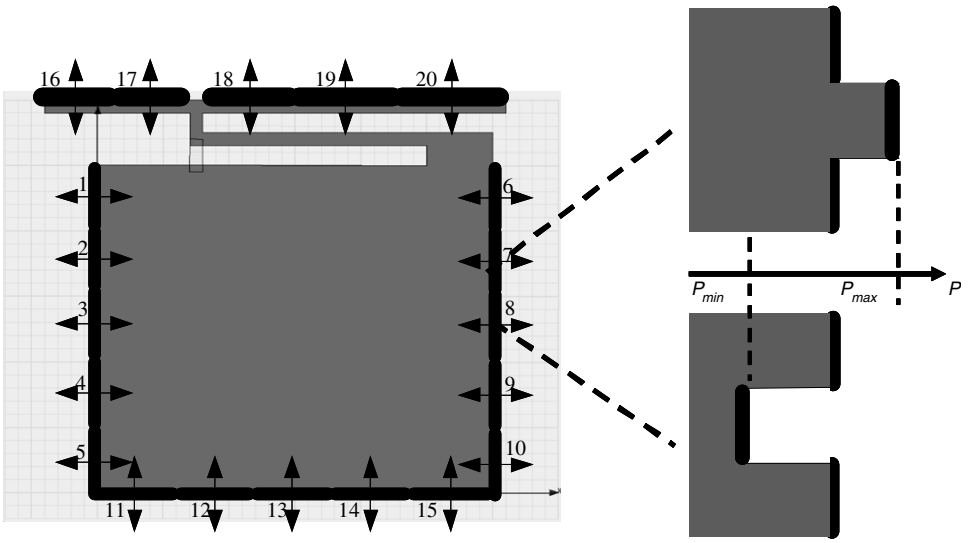

Fig. 5. The original geometry of examined antenna and the partitioned segments. The black rectangular frame near the top line is the contact for input excitation. The partitioned segments allow us to perturb the geometry without spatial limitation in a specific region. The Zoom-in plot shows the diagram for the segment movement.

P_4 can represent the movements of different segments, and can be seen in Fig. 4. In the GA with simulation-based antenna optimization problem, all unknowns to be extracted are floating-point numbers. We transform these continuous floating-point numbers into discrete steps (*Psteps*) through step function, as shown in Eq. (17), instead of real numbers, and we encode the discrete steps as genes on chromosomes. The discrete steps show the strongly combinatorial properties, and we have found that this representation has better results in crossover and mutation.

$$P_{value} = P_{\min} + Psteps \frac{P_{\max} - P_{\min}}{R_{esolution}}, \tag{17}$$

where the P_{value} is the real value of the movement or width which is a float-point number. $P_{\min}$ and $P_{\max}$ are the minimum and maximum values of each parameter, and $R_{esolution}$ defines the magnitude of single step to vary of a parameter. Then, the step function *Psteps* can be encoded, and the real number problem is translated into genes. Here the binary values representation is used. To show how to apply the encoding method to fine tune the antenna geometry, the bottom one of the Fig. 4 presents the movements of one partitioned segment.

In this work, the movements of segments satisfy the following rules. Each segment from 1 to 15, as shown in Fig. 5, can shift inward or outward within a specified range, while the value of parameter 16 to 20 indicates the width of the top line. And they can be efficiently achieved via the encoding method.

(3) Fitness Evaluation

The fitness evaluation calculates the fitness score for each chromosome. The fitness score can be seen as the accommodation status of each chromosome in the current environment. In our optimization scheme, the user-defined specification for return loss is used as the fitness. Due to the different operation frequencies, the return losses within the bandwidth around those operation frequencies are taken into account. Here we use the difference of the return loss between the adjusted antenna and the specification as the fitness. It can be rewritten in the following formulation

$$F = \sum_{i=1}^{\#freq} \left(return\_loss_i - RL_{th,i} \right), \tag{18}$$

where F is the fitness, the $return\_loss_i$ denotes the optimized return loss at requested frequency i, $RL_{th,i}$ means the specific return loss needed to be achieved at frequency i, and *#freq* is the number of requested frequencies. The smaller fitness reflects the optimized return loss is close to the specification.

(4) Selection Method

After the fitness score for each chromosome is obtained, a selection method selects chromosomes that will stay in the population and breed the next generation. There are many selection schemes, such as ranking selection, roulette wheel selection, and tournament selection. The ranking selection selects chromosomes with the rule of first-rate score. The roulette wheel selection gives each chromosome a different chosen rate by the average score and the fitness scores of each chromosome; and the tournament selection chooses several pairs of chromosomes and selects the better one of each pair. In this work, the ranking selection is chosen for its simplicity.

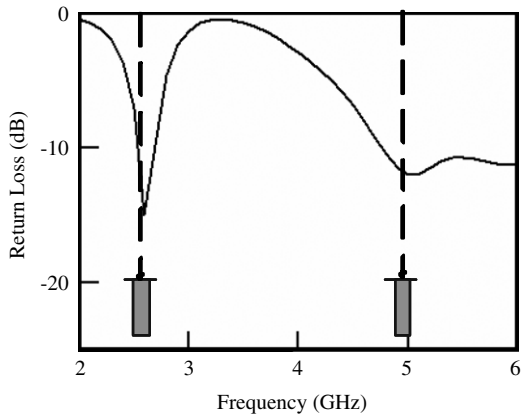

Fig. 6. The return loss of the original geometry and requested return loss. The goal is to make the return loss reach the gray region along the two dash lines. The original antenna is a dual-band design but has only one clear band at 2.6 GHz. The return loss on the frequency 4.9 GHz still has room for performance improvement.

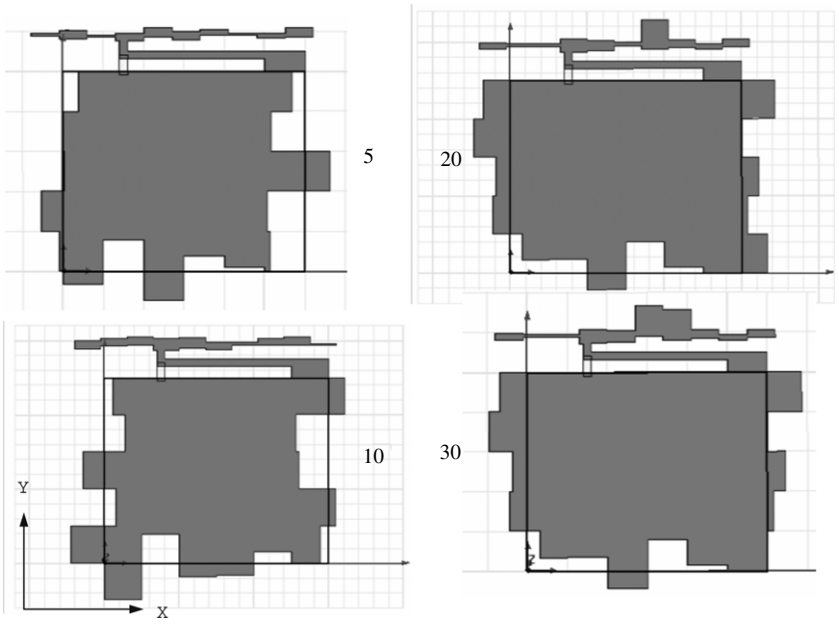

Fig. 7. Some generations of antenna patterns in GA procedure.

(5) Crossover Procedure and Mutation Scheme

When selection has been carried out, we will perform the crossover procedure. Crossover procedure mates two chromosomes selected by the selection method, to generate new chromosomes. To generate offspring, the crossover operator gives a few cuts on the parent chromosomes and exchanges the genes. In this work, the single-point cut crossover scheme is adopted. After the crossover procedure, a certain rate of the newborn chromosomes mutates into another different chromosomes. The mutation rate is typically less than 1%. The mutation scheme may act in different ways. In the proposed method, it increases the mutation rate when the behavior tends to a saturation situation, and decreases the mutation rate when the population achieves a high diversity. Both crossover and mutation are shown in Fig. 4.

After the above steps are complete, the GA evaluates the next population and continues until certain stop criteria is reached.

4. Results and discussion

Fig. 5 shows the original shape of the examined antenna. The studied structure is a Z-shaped antenna and has radiation elements and ground plane on the same plane. As shown in Fig. 5, the top line is the ground plane, the bottom rectangle

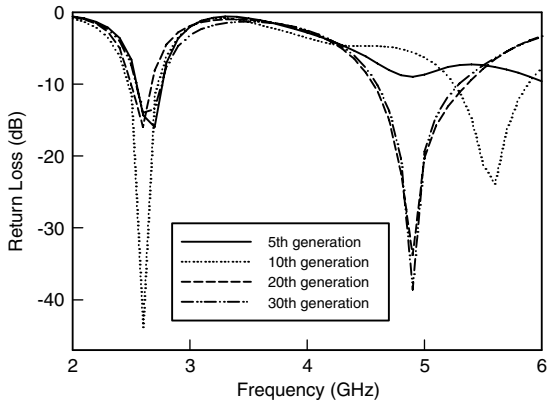

Fig. 8. The return losses corresponding to generations of antenna patterns in GA procedure.

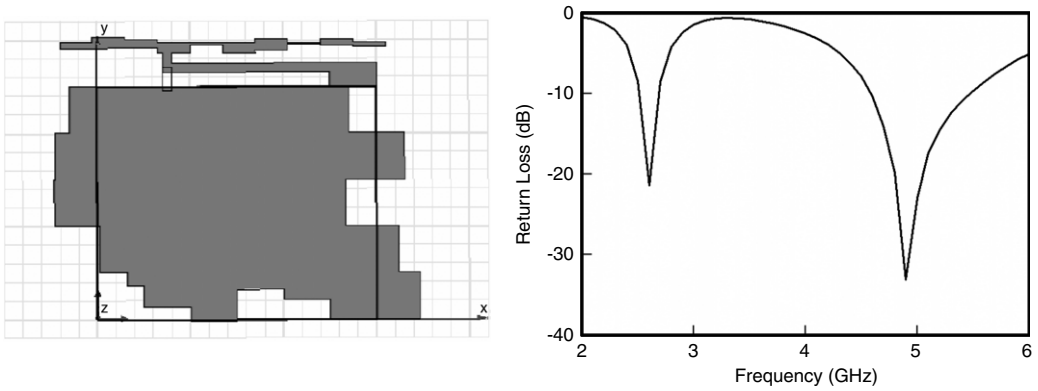

Fig. 9. (a) An optimized geometry of the examined antenna after our optimization scheme. The geometry of radiation element is obviously tuned by GA to enhance the transmitting and receiving properties of the antenna. (b) The return loss of the optimized antenna.

represents the radiation element, and the segments 1–20 are the partitions for evolution. Fig. 6 shows the return loss of the original antenna. The dual operating frequencies are set to 2.6 and 4.9 GHz. The frequency 2.6 GHz is referred as the "S-band" used for mobile broadcasting and the frequency 4.9 GHz is used by the 802.11a WLAN protocol. Our target is to improve the return loss for both operating frequencies — 2.6 and 4.9 GHz. It means the return loss will reach the gray region at those two frequencies along the dash lines in the figure. Apply GA to search the better antenna patterns automatically. The antenna patterns in some generations are shown in Fig. 7. Fig. 8 shows the corresponding return losses for the antenna patterns in each generation. The number on the subplots in Fig. 7 represents the number of generations in GA procedure. Fig. 8 shows that the return loss of the second band has been improved as the number of generations increase. When the antenna pattern generated by GA satisfies the design specifications, it will be the optimized pattern. Fig. 9(a) shows the optimized geometry, and Fig. 9(b) illustrates the corresponding result. Compared with Fig. 6, the return loss on the frequencies of 2.6 and 4.9 GHz is down to 20 dB for the optimized antenna, which is a significant improvement. As shown in Fig. 5, the original Z-shape antenna is located in the xy-plane and its normal vector is in the z direction.

For the radiation property of the desired antenna, we want to hold the omidirectional radiation in the xz-plane after the proposed optimization scheme. The radiation patterns are calculated by solving the Maxwell's equations. As shown in Figs. 10 and 11, the original antenna has omidirectional gain pattern in the xz-plane at 2.6 GHz and 4.9 GHz. After optimization, the gain patterns are still omidirectional in the xz-plane at the dual operating frequencies, as shown in Figs. 12 and 13. From Figs. 10–13, we notice that the gain of the optimized antenna is close to that of the original one at both operating frequencies, which reserves the omidirectional radiation property. But the return losses are obviously improved after the optimization.

To analyze the convergence of the proposed intelligent approach, here the convergence under different mutation rates and population sizes are further examined. The parameter setting for GA in this work is as follows: crossover rate is 0.6, selection rate is 0.6, new spring rate is 0.3. Fig. 14 shows the fitness score convergence behavior for the antenna optimization with different mutation rates, where the population size used in this testing is equal to 5. We note that generations increase, and the results suggest that the high mutation rates over 0.3 keep the population diverse and have better evolutionary

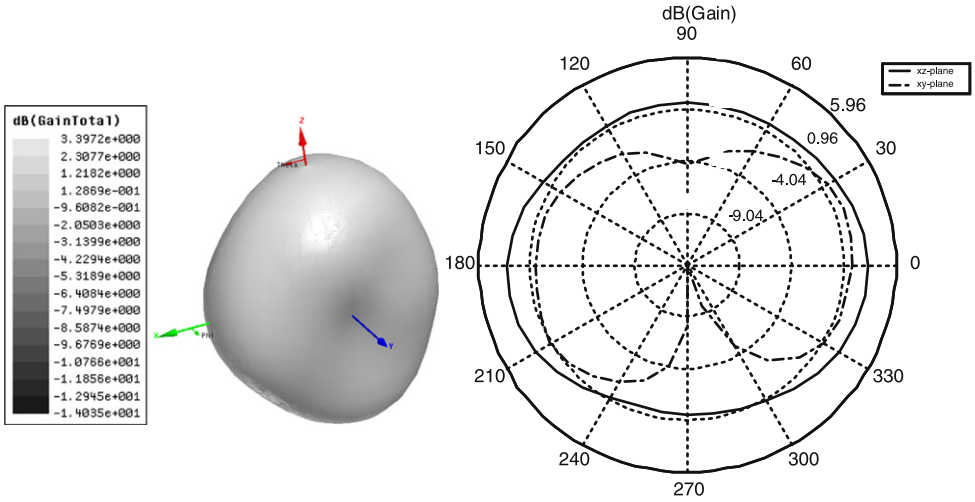

Fig. 10. The gain pattern for the original antenna at 2.6 GHz. The left object is the 3D gain pattern. The right one is the 2D gain pattern. The solid line represents the gain pattern in the xz-plane, and the dashed line is the gain pattern in the xy-plane. The original antenna has an omidirectional gain pattern of 2.6 GHz.

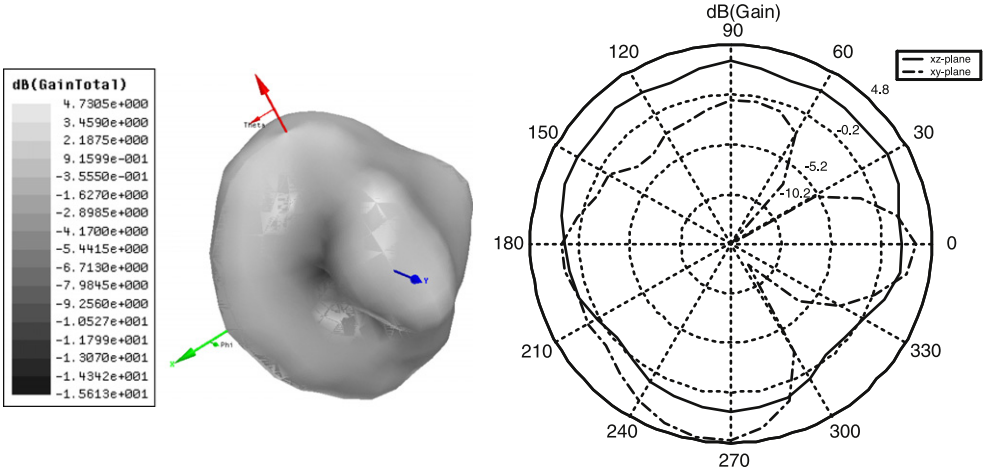

Fig. 11. The gain pattern for the original antenna at 4.9 GHz. The left object is the 3D gain pattern. The right one is the 2D gain pattern. The solid line represents the gain pattern in the xz-plane, and the dashed line is the gain pattern in the xy-plane. The original antenna has a near omidirectional gain pattern of 4.9 GHz.

results. Fig. 15 shows the fitness score versus the extraction time; three different population sizes are compared using the same mutation rate 0.6. The results indicate that the best performance is achieved when the population size of 5 is adopted.

5. Conclusions

In this paper, a simulation-based optimization method for the design of an antenna has been presented. GA works well for the antenna design automation on our UOF, and communicated with an external numerical EM solver. This method minimizes the return loss under the frequencies 2.6 and 4.9 GHz. Improved return loss is observed, and the effect of this method for the optimized configuration is examined and discussed. The receiving and transmitting properties of the optimized antenna are simulated and the resulting gain pattern is still omidirectional in the xz-plane. Furthermore, the gain is close to the original antenna. The optimized antenna has a gain pattern as good as the original one, but the operating frequencies are enhanced for dual band design. To validate this method, more antennas with different operating frequencies will be examined, such as wire antenna, patch antenna, broadband antenna, etc. Furthermore, UOF also has capability to connect with other external software through the script file, which can generate the antenna geometry. We believe that this optimization method can benefit the RF antenna design applied for mobile broadcasting and the 802.11a WLAN.

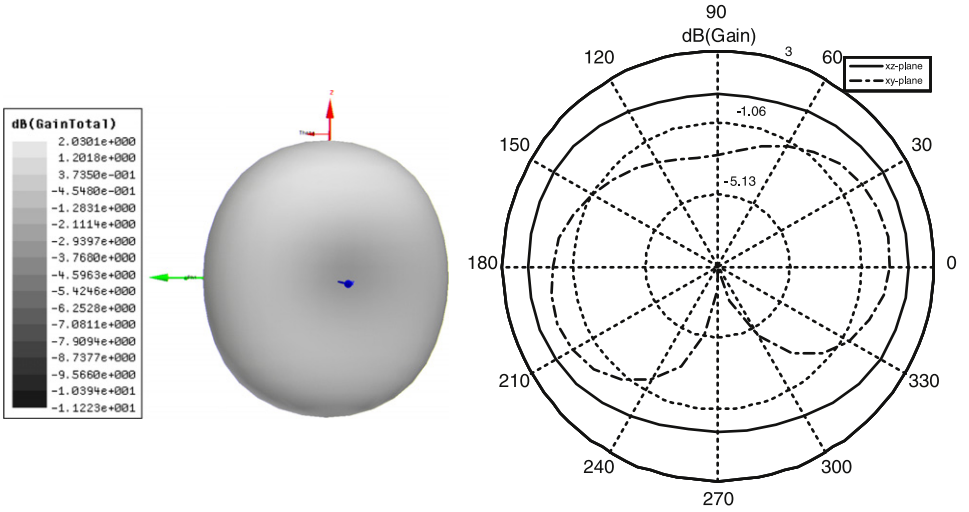

Fig. 12. The gain pattern for the optimized antenna at 2.6 GHz. The left object is the 3D gain pattern. The right one is the 2D gain pattern. The solid line represents the gain pattern in the xz-plane, and the dashed line is the gain pattern in the xy-plane. The optimized antenna holds the near omidirectional gain pattern at 2.6 GHz.

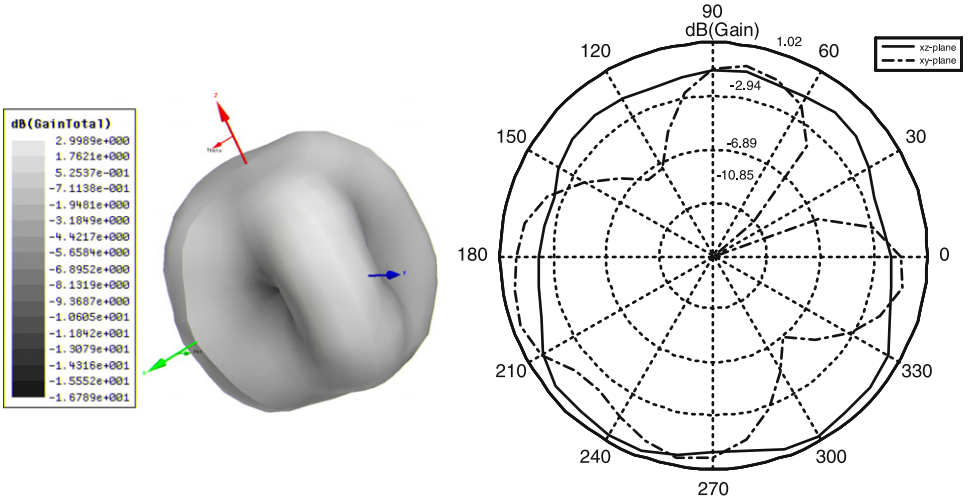

Fig. 13. The gain pattern for the optimized antenna at 4.9 GHz. The left object is the 3D gain pattern. The right one is the 2D gain pattern. The solid line represents the gain pattern in the xz-plane, and the dashed line is the gain pattern in the xy-plane. The optimized antenna has a near omidirectional gain pattern at 4.9 GHz.

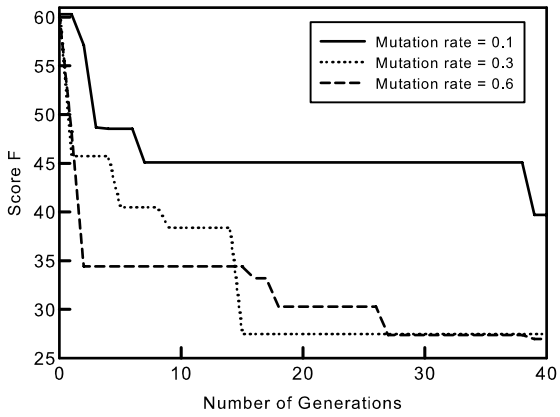

Fig. 14. A plot of fitness score convergence vs the number of generations with respect to different mutation rates.

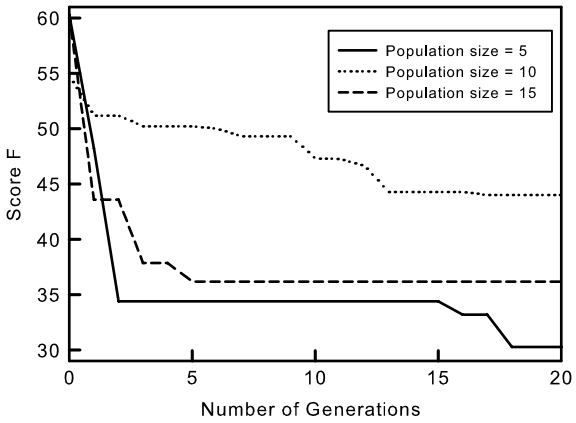

Fig. 15. A plot of fitness score convergence vs the number of generations with respect to different population sizes.

Acknowledgments

This work was supported in part by National Science Council (NSC), Taiwan under Contract NSC-96-2221-E-009-210 and NSC-97-2221-E-009-154-MY2.

References

[1] A. Boag, A. Boag, E. Michielssen, R. Mittra, Design of electrically loaded wire antenna using genetic algorithm, IEEE Trans. Antennas and Propagation 44 (1996) 687–695.
[2] N. Cohen, Fractal coding in genetic algorithm (GA) antenna optimization, IEEE Antennas and Propag. Society International Symposium 3 (1997) 1692–1695.
[3] W. Comisky, J.R. Koza, J. Yu, Automatic synthesis of a wire antenna using genetic programming, in: Late Breaking Papers at the 2000 Genetic and Evolutionary Computation Conference, Las Vegas, Nevada, 2000, pp. 179–186.
[4] F. Castellana, F. Bilotti, L. Vegni, Automated dual band patch antenna design by a genetic algorithm based numerical code, IEEE Antennas Propag. Society International Symposium 4 (2001) 696–699.
[5] J.P. Gianvittorio, Y. Rahmat-Smaii, Fractal antennas: A novel antenna miniaturization technique, and applications, IEEE Antennas Propag. Mag. 44 (2002) 20–36.
[6] D.H. Werner, S. Ganguly, An overview of fractal antenna engineering research, IEEE Antennas Propag. Mag. 45 (2003) 38–57.
[7] F.J. Villegas, T. Cwik, Y. Rahmat-Samii, M. Manteghi, A parallel electromagnetic genetic-algorithm optimization (EGO) application for patch antenna design, IEEE Trans. Antennas and Propagation 52 (2004) 2424–2435.
[8] J.D. Lohn, D.S. Linden, G.S. Hornby, A. Rodriguez-Arroyo, S.E. Seufert, B. Blevins, T. Greenling, Evolutionary design of a single-wire circularly-polarized X-band antenna for NASA's space technology 5 mission, IEEE Antennas Propag. Society International Symposium 2B (2005) 267–270.
[9] N. Jin, Y. Rahmet-Samii, Parallel particle swarm optimization and finite difference time-domain (PSO/FDTD) algorithm for multiband and wide-band patch antenna designs, IEEE Trans. Antennas and Propagation 53 (2005) 3459–3468.
[10] H.T. Chou, Y.C. Hou, W.J. Liao, A dual band patch antenna design for WLAN and DSRC applications based on a genetic algorithm optimization, Electromagnetics 27 (2007) 253–262.
[11] J.R. Koza, S.H. Al-Sakran, L.W. Jones, G. Manassero, Automated synthesis of a fixed-length loaded symmetric dipole antenna whose gain exceeds that of a commercial antenna and matches the theoretical maximum, in: Proceedings of the 9th Annual Conference on Genetic and Evolutionary Computation, 2007, pp. 2074–2081.
[12] E.E. Altshuler, D.S. Linden, Wire-antenna designs using genetic algorithms, IEEE Antennas Propag. Mag. 39 (1997) 33–43.
[13] A.J. Kerkhoff, R.L. Rogers, H. Ling, Design and analysis of planar monopole antennas using a genetic algorithm approach, IEEE Trans. Antennas and Propagation 52 (2004) 2709–2718.
[14] W.-C. Liu, Design of a multiband CPW-fed monopole antenna using a particle swarm optimization approach, IEEE Trans. Antennas and Propagation 53 (2005) 3273–3279.
[15] Y. Li, S.-M. Yu, Y.-L. Li, Electronic design automation using a unified optimization framework, Math. Comput. Simul. 79 (2008) 1137–1152.
[16] Y. Li, S.-M. Yu, A unified optimization framework for real world problems, in: T. Simos, et al. (Eds.), Lecture Series on Computer and Computational Sciences, in: Recent Progress in Computational Sciences and Engineering, vol. 7, Brill Academic Publishers, 2006, pp. 816–819.
[17] Y. Li, Y.-Y. Cho, Intelligent BSIM4 model parameter extraction for sub-100 nm MOSFET era, Japan J. Appl. Phys. 43 (2004) 1717–1722.
[18] Y. Li, Y.-Y. Cho, C.-S. Wang, K.-Y. Huang, A genetic algorithm approach to InGaP/GaAs HBT parameters extraction and RF characterization, Japan. J. Appl. Phys. 42 (2003) 2371–2374.
[19] Y. Li, C.-T. Sun, C.-K. Chen, A floating-point based evolutionary algorithm for model parameters extraction and optimization in HBT device simulation, in: L. Rutkowski, J. Kacprzyk (Eds.), Advances in Soft Computing - Neural Networks and Soft Computing, Physica-Verlag, 2003, pp. 364–369.
[20] J. Holland, Adaptation in Natural and Artificial Systems, University of Michigan Press, Ann Arbor, Mich., 1975.
[21] R. Salomon, Evolutionary algorithms and gradient search: Similarities and differences, IEEE Trans. Evolutionary Computation 2 (1998) 45–55.
[22] P. Bhartia, I. Bahl, R. Garq, A. Ittipiboon, Microstrip antenna design handbook, Norwood, MA, Artech House, 2000.
[23] Scott Santarelli, Tian-Li Yu, David E. Goldberg, Edward Altshuler, Teresa O'Donnell, Hugh Southall, Robert Mailloux, Military antenna design using simple and competent genetic algorithms, Math. Comput. Modeling 43 (2006) 990–1022.
[24] S.-M. Yu, Y. Li, A computational intelligent optical proximity correction for process distortion compensation of layout mask in subwavelength era, in: Abstracts of the 10th International Workshop on Computational Electronics, 2004, pp. 179–180.
[25] S.-M. Yu, Y. Li, A pattern-based domain partition approach to parallel optical proximity correction in VLSI designs, in: Proceedings of IEEE Parallel and Distributed Processing Symposium, 2005.
[26] S.-M. Yu, Y. Li, A parallel intelligent OPC technique for design and fabrication of VLSI circuit, Technical Proceedings of the 2005 NSTI Nanotechnology Conference and Trade Show 3 (2005) 724–727.
[27] Y. Li, Intelligent BSIM 4 model parameter extraction for sub-100 nm MOSFET era, Japan. J. Appl. Phys. 43 (2004) 1717–1722.

[28] Y. Li, Y.-Y. Cho, An automatic parameter extraction technique for advanced CMOS device modeling using genetic algorithm, Microelectron. Eng. 84 (2007) 206–272.
[29] Y. Li, S.-M. Yu, A coupled-simulation-and-optimization approach to nanodevice fabrication with minimization of electrical characteristics fluctuation, IEEE Trans. Semicond. Manuf. 20 (2007) 432–438.
[30] J. Jin, The Finite Element Method in Electromagnetics, 2nd ed., John Wiley & Sons, NY, 2002.
[31] B. Engquist, A. Majda, Absorbing boundary conditions for the numerical simulation of waves, Proceedings of the National Academy of Sciences 74 (1977) 629–651.
[32] J.M. Jin, N. Lu, Application of adaptive absorbing boundary condition to finite element solution of three-dimensional scattering, IEE Proc.-Microwaves, Antennas and Propagation 143 (1996) 57–61.
[33] J.M. Jin, J.L. Volakis, V.V. Liepa, An engineer's approach for terminating finite element meshes in scattering analysis, IEEE Antennas Propag. Society International Symposium 2 (1991) 1216–1219.
[34] J.P. Berenger, A perfectly matched layer for the absorption of electromagnetic waves, J. Comput. Phys. 114 (1994) 185–200.
[35] J.P. Berenger, Three-dimensional perfectly matched layer for the absorption of electromagnetic waves, J. Comput. Phys. 127 (1996) 363–379.
[36] W.L. Stutzman, Antenna Theory and Design, John Wiley & Sons, NY, 1998.
[37] http://www.ansoft.com/products/hf/hfss/.
[38] http://www.feko.info/.
[39] http://www.zeland.com/.